Intrapulmonary Delivery of XCL1-Targeting Small Interfering RNA in Mice Chronically Infected with *Mycobacterium tuberculosis*

Adrian G. Rosas-Taraco[1]*, David M. Higgins[1], Joaquín Sánchez-Campillo[1‡], Eric J. Lee[1], Ian M. Orme[1], and Mercedes González-Juarrero[1]

[1]Mycobacteria Research Laboratories, Department of Microbiology, Immunology, and Pathology, Colorado State University, Fort Collins, Colorado

Mice infected for 60 days with *Mycobacterium tuberculosis* were treated with aerosolized XCL1-targeting small interfering RNA (siRNA) to induce local and transient suppression of XCL1/lymphotactin (an important chemokine in tuberculoid granuloma formation). The local pulmonary siRNA therapy resulted in a 50% decrease in the total amount of *xcl1* gene transcripts at 3 days, and 40 to 50% protein suppression 3 and 5 days after treatment. Reduced XCL1 expression in the lungs was associated with decreased numbers of T lymphocytes, reduction in the IFN-γ response, disorganized granulomatous lesions, and higher fibrosis when compared with control mice treated with either PBS or nontargeting siRNA. This indicates that a transient but strong modulation of the production of XCL1 in the lungs has a significant effect on the influx of IFN-γ–secreting T cells, as well as local pathology, but without significantly altering containment of the infection.

Keywords: tuberculosis; small interfering RNA; lymphotactin; XCL1; aerosol delivery

CLINICAL RELEVANCE

We demonstrate, for the first time, in a murine tuberculosis model, that it is possible to modulate the local environment and the lung immunopathology using small interfering RNA. Currently, a variety of acute and chronic lung diseases have been shown to have altered expression of cytokines/chemokines or other important factors, many of which could be directly involved in lung pathology. Therefore, workers in many other respiratory diseases will clearly be able to use the approaches described here to elucidate the role of different molecules in pathogenesis. These same approaches may be exploited as immunotherapeutic alternatives for respiratory diseases.

Up to now, *in vivo* studies addressing the role of specific components of the immune response during chronic infection with *Mycobacterium tuberculosis* were limited to the use of gene-targeted knockout mice or systemic antibody and drug delivery. Although these methods provided important information in regards to tuberculosis infection, they do not allow for targeted examination of the lung-unique environment. Furthermore, gene knockout mice have the deficiency from the onset, thus not allowing more temporal manipulation of the immune response. For that reason, here, we tried an innovative approach in which newly developed immunotherapeutic molecules were applied directly to the lungs. Specifically, we transiently changed the lung immune environment by delivery of small interfering RNA (siRNA) transcripts.

siRNA is a technology being used to evaluate the function of a variety of genes by transient silencing of mRNA expression. This new technology has been used as a therapeutic procedure to treat a variety of genetic, viral, and cancer-related diseases (1). It has demonstrated therapeutic benefits after both local and systemic administration into subcutaneous tissue, muscle, eye, and the central nervous system (2, 3). The major challenge of using siRNA as an immunotherapy is to deliver it into tissues and then into the cytoplasm of cells. Exceptions to this are the mucosal tissues and the lung. In these tissues, it has been demonstrated that siRNA uptake is extremely efficient and occurs even in the absence of transfection reagents (4–7). We took advantage of this, and developed a procedure to transiently block expression of proteins by using a noninvasive procedure for intrapulmonary delivery of aerosolized siRNA. Using this approach we studied changes in the immunopathology in mice chronically infected with *M. tuberculosis*.

Tuberculosis is a global problem caused by infection with the *M. tuberculosis* bacilli. At the present time, one third of the world population has been exposed to this bacillus, and two million people die every year of tuberculosis (8). Activation of antigen-presenting cells and T lymphocytes to produce type 1 T helper cytokines is an essential step to limiting the multiplication of *M. tuberculosis* (9, 10). Primed T cells are then recruited to the lungs, driven by chemokine gradients, where they deliver IFN-γ to infected cells. Despite the presence of a strong type 1 T helper cell–type immune response in the lungs, the host is unable to completely eliminate the bacteria. As a result, an inflammatory process ensues in which the surviving bacteria persist for long periods of time (11).

One of the chemokines known to participate in the formation of the lung granuloma is XCL1, also known as lymphotactin or ATAC. Through the use of intrapulmonary aerosolized delivery, we recently demonstrated that murine-recombinant XCL1 reduced the number of IFN-γ–secreting CD4 T cells within *M. tuberculosis*–infected lungs (12). Our results above allowed us to hypothesize that the capacity or presence of CD4 T-cell populations producing IFN-γ could be influenced in the lungs by the chemokine, XCL1. During this study, however, we were unable to evaluate this further, because previous experimental approaches used to suppress expression or block proteins (gene

(*Received in original form September 22, 2008 and in final form December 9, 2008*)

* Present affiliation: Departamento de Inmunología, Facultad de Medicina. Universidad Autónoma de Nuevo León, Monterrey, Nuevo León, México

‡ Present affiliation: Departamento de Histología y Anatomía Patológica Comparadas, Universidad de Murcia, Murcia, Spain

This work was supported by National Institutes of Health grant AI-44072 (I.M.O.).

Correspondence and requests for reprints should be addressed to Mercedes González-Juarrero, Ph.D., Department of Microbiology, Immunology, and Pathology, Colorado State University, Fort Collins, CO 80523-1682. E-mail: malba@mail.colostate.edu

Am J Respir Cell Mol Biol Vol 41. pp 136–145, 2009
Originally Published in Press as DOI: 10.1165/rcmb.2008-0363OC on December 18, 2008
Internet address: www.atsjournals.org

knockout or blockage by antibody delivery) were unavailable or too expensive. To test our hypothesis, we then used an siRNA sequence targeting XCL1 and delivered it in an aerosol form by the intrapulmonary route. With this procedure, we were able to demonstrate that local delivery of XCL1-targeting siRNA was capable of transiently blocking XCL1 expression during a chronic pulmonary infection with *M. tuberculosis.* Thereafter, we followed changes in the course of the pulmonary immune responses and pathogenesis of the disease. Our study design not only demonstrated the role of XCL1 during the course of the immune response to pulmonary *M. tuberculosis* infection, but also provided evidence that a transient suppression of XCL1 using a single intrapulmonary delivery of siRNA during chronic infection with *M. tuberculosis* has a long-term effect in the course of pulmonary immunopathology.

MATERIAL AND METHODS

Mice and Experimental Infections

Specific pathogen-free female C57BL/6 (6–8 weeks old) were purchased from the Jackson Laboratories (Bar Harbor, ME). Mice were maintained in the biosafety level 3 biohazard facilities at Colorado State University, and were given sterile water, mouse chow, bedding, and enrichment food for the duration of the experiments. All experimental protocols used in this study were approved by the Animal Care and Use Committee of Colorado State University.

Mice were infected by low-dose aerosol challenge with *M. tuberculosis* Erdman strain using a Glass-Col (Terre Haute, IN) aerosol generator calibrated to deliver 50–100 bacteria into the lungs. The success of bacterial deposition in the lungs was demonstrated 24 hours after aerosol infection by determining the number of bacteria in the lungs from five mice by plating serial dilutions of the organ homogenates on nutrient 7H11 agar and counting CFU after a 3-week incubation at 37°C (13). Bacterial loads were also evaluated in lungs of infected mice receiving siRNA. Lungs from mice ($n = 5$) in the same groups were harvested and processed for quantitative RT-PCR (qRT-PCR), histological, cell population, or ELISA analysis.

XCL1-Targeting siRNA

XCL1-targeting siRNA was commercially predesigned from the gene number access for *xcl-1* (NM_008510) by Qiagen (Valencia, CA). siRNA was chosen with the sequence (sense) r(GGG CCA GUA CCA GAA AGA A)dTdT and (antisense) r(UUC UUU CUG GUA CUG GCC C)dTdG. The sequence of the *xcl-1* gene targeted by this siRNA is CAG GGC CAG TAC CAG AAA GAA. XCL1-targeting siRNA was tagged with Alexa Fluor 488. The siRNA was commercially produced and purchased from Qiagen. Nontargeting siRNA (AllStars negative control siRNA) was included as a negative control and was also obtained from Qiagen.

Intrapulmonary Delivery of siRNA

Mice were treated by the intrapulmonary route following a previously described protocol (14). Briefly, mice were anesthetized by intraperitoneal injection of 100 mg/kg and 10 mg/kg body weight of ketamine and xylazine, respectively. The mice were suspended by their upper teeth on a platform slanted at a 45° angle. The tongue was gently pulled out with padded tweezers and a small laryngoscope (Penn-Century, Inc., Philadelphia, PA) was used to visualize the trachea. An intratracheal microsprayer (Penn-Century, Inc.) was inserted into the trachea and used to deliver 50 μl of aerosolized sample into the lungs. The microsprayer was immediately withdrawn and the mouse was removed from the platform. Each group of mice ($n = 5$) received one dose of 5, 10, or 15 μg of XCL1-targeting siRNA, nontargeting siRNA, or PBS. After intrapulmonary delivery, mice were monitored until they recovered from anesthesia.

Furthermore, using a Xenogen IVIS Imaging System (Caliper Life Sciences, Hopkinton, MA), we demonstrated that the aerosolized intrapulmonary delivery of fluorescent molecules using this noninvasive protocol was evenly distributed in all five lobes of the lungs (data not shown). This observation was also reported in other studies (15, 16).

Mice were killed at 3, 5, or 180 days after treatment. An additional group of mice was used to determine colocalization of fluorescent siRNA in several tissues 24 hours after delivery. For this purpose, siRNA-Alexa 488 was delivered by the intrapulmonary route, as described above, and, 24 hours after delivery, the lung, spleen, liver, or draining lymphoid tissue were prepared as cell suspensions using a previously described protocol (17); detection of fluorescence in each sample was determined using flow cytometric analysis.

Sample Preparation

Mice were killed by CO_2 asphyxiation, and the thoracic cavity was opened. Diaphragmatic lobe was collected for histology and immunohistochemistry (IHC) analysis. Thereafter, the lungs were perfused with an ice-cold solution containing PBS and heparin (50 U/ml; Sigma-Aldrich, St. Louis, MO) through the pulmonary artery. The left lobe of the lung was dissected and incubated with complete RPMI (cRPMI media) for flow cytometry and nitric oxide analysis. The right inferior lobe was placed into 1 ml of sterile PBS for ELISA assays. The right mid-lobe was placed into 1 ml Trizol reagent for qRT-PCR analysis. Finally, the right superior lobe was place into 1 ml of sterile saline solution for viable count analysis.

ELISA Assays

Each lobe was placed into 1 ml sterile PBS and homogenized using a tissue homogenizer. Thereafter, the tissue homogenates were frozen and stored at −80°C until they were used for ELISA. The samples were screened in triplicate by ELISA following manufacturer's protocol for XCL1 (R&D Systems, Minneapolis, MN) and IFN-γ (eBioscience, San Diego, CA) detection. The concentrations of XCL1 and IFN-γ were calculated using a standard curve of their respective recombinant molecules.

qRT-PCR

The lung lobe was homogenized in Trizol and frozen at −80°C immediately. RNA was extracted following the manufacturer's protocol for Trizol (Invitrogen, Carlsbad, CA). DNA was digested with RQ1 RNase-free DNase (Promega, Madison, WI), and RNA was reisolated with Trizol. Finally, concentration of RNA in each sample was measured by spectrophotometry, and the RNA was reverse transcribed with M-MuLV (New England BioLabs, Ipswich, MA) and random hexamers (Roche, Basel, Switzerland). Real-time PCR was performed using 5 μl of cDNA and platinum SYBR green qPCR SuperMix-UDG (Invitrogen) in iQ5 thermocycler (Bio-Rad, Hercules, CA) to evaluate relative mRNA expression of XCL1 and inducible nitric oxide synthase (iNOS), GAPDH was used to standardize gene expression. The primer sequences used were: for XCL1, forward, 5′ GCAAGACCTCAGCCATGAGA 3′, and reverse, 5′ GCC GCTGGGTTTGTAAGTTC 3′; for iNOS, forward, 5′ CAG CTGGGCTGTACAAACCTT 3′, and reverse, 5′ CATTG GAAGTGAAGCGTTTCG 3′; for transforming growth factor (TGF)-β, forward, 5′GACCCTGCCCCTATATTTGGA 3′, and reverse, 5′GCCCGGGTTGTGTTGGT 3′; and for GAPDH, forward, 5′ TCACCACCATGGAGAAGGC 3′, and reverse, 5′

GCTAAGCAGTTGGTGGTGCA 3′. Amplification conditions were as follows: 50°C for 2 minutes, 95°C for 2 minutes, and 40 cycles of denaturation at 95°C for 15 seconds, annealing and extension at 58°C for 30 seconds. Specificity was verified by melt-curve analysis. XCL1 and iNOS mRNA levels were normalized with GAPDH levels using the ΔΔCt ($\Delta Ct_{sample} - \Delta Ct_{GAPDH}$) method to calculate relative changes.

Flow Cytometric Analysis

The left lung lobe was digested using collagenase XI (0.7 mg/ml; Sigma-Aldrich) and type IV bovine pancreatic DNase (30μg/ml; Sigma-Aldrich) for 30 minutes at 37°C. The digested lungs were further disrupted by gently pushing the tissue through a cell strainer (BD Biosciences, San Jose, CA). Red blood cells were lysed with Gey's solution, washed, and resuspended in cRPMI. Total cell numbers per lung were determined using counting beads (BD Biosciences). Cell suspensions from each individual mouse were incubated with monoclonal antibodies (mAbs) labeled with phycoerythrin, peridinin chlorophyll-a protein, or allophycocyanin. After washing the cells with PBS containing 2% FBS and 0.1% sodium azide (Sigma-Aldrich), the cells were incubated with mAbs against CD4 (Rat IgG2a, clone RM4-5), CD8 (Rat IgG2a, clone 53-6.7), and corresponding isotype antibodies, and incubated at 4°C for 30 minutes in the dark. Then, the cells were permeabilized with Perm Fix/Perm Wash (BD PharMingen, San Diego, CA), and stained for intracellular IFN-γ (Rat IgG1, clone XMG1.2). The remaining mAbs were purchased from BD PharMingen or eBioscience. Data acquisition and analysis for this study were done using an LSRII (BD Biosciences) and FACSDiva software (BD Biosciences), respectively. Analyses were performed with an acquisition of at least 100,000 total events in the cell gate.

Histopathology Analysis

The diaphragmatic lobe of the lungs of each mouse was placed into histology cassettes and fixed in formalin-free Zn reagent (BD Bioscience, Mountain View, CA). After 48 hours, samples were inactivated inside the BSL-3 laboratory and then processed using standard histological protocols. Histopathological evaluation was done in tissue sections from each sample stained with hematoxylin and eosin (H&E) or Masson's trichromic stain.

Quantitative Image Analysis of Fibrosis Using Masson's Trichrome Staining

The extent of fibrosis in accumulating macrophages or granulomatous lesions was quantified by Masson's trichrome staining and computer-assisted image analysis, as previously reported (18, 19). Images were taken using an Olympus BX41 microscope and DP70 camera (Olympus, Center Valley, PA). Image data was analyzed on Adobe Photoshop CS (Adobe, San Jose, CA). All images were obtained using a 20× objective. Camera settings were under manual control and held constant to produce comparable conditions for image acquisition. For each group ($n = 5$), 25 randomly selected images of accumulating macrophages or granulomatous lesions were captured by a blinded researcher. Positive blue signal, indicating collagen, was selected based on its color ranges, and the proportional area in each image was quantified using the Photoshop histogram tool and expressed as a percentage of the image.

IHC

After removing the lungs from the pulmonary cavity, the lobes from each group of mice were placed in a histology cassette and incubated at room temperature in formalin-free zinc fixative (BD Pharmingen) for 48 hours. Immediately after, the samples were dehydrated on alcohol gradients and embedded in paraffin. Paraffin-embedded blocks from each group of mice were cut in 5- to 7-μm-thick sections. Thereafter, the paraffin was removed from the tissue sections using EZ-DeWax solution (Biogenex Lab, San Ramon, CA) and rehydrated. Tissue-endogenous peroxidase was blocked using methanol containing 0.3% H_20_2 for 20 minutes, and the sections were washed. Unspecific binding of the antibody was blocked using 3% BSA in PBS for 30 minutes. After this step, each section was incubated overnight at 4°C with a primary antibody (TGF-β, 1:75, and IL-4, 1:50; Santa Cruz Biotechnology, Santa Cruz, CA). After washing the slides three times for 5 minutes in PBS at room temperature, the slides were incubated again with the appropriate biotinylated secondary antibody for 1 hour at room temperature. The specific antibody binding reaction was amplified by incubation with ABC development system (Vector Laboratories, Burlingame, CA) for 30 minutes at room temperature. After the amplification step, the slides were washed and incubated again for 5 minutes with the chromogen substrate for horseradish peroxidase, aminoethycarbazole (Vector Laboratories). Finally the slides were counter stained using hematoxylin for 10 seconds (Vector Laboratories) and, after washing with tap water, the slides were mounted for microscopic observation using aqueous mounting media crystal/mount (Biomedia Corp., Foster City, CA).

Viable Count

Each lobe was placed into 4 ml of sterile saline solution and homogenized. Serial dilutions were done in sterile saline solution, and 0.1 ml of each solution was poured onto nutrient 7H11 agar plates. The agar plates were incubated for 21 days at 37°C. The bacterial load was determined by counting CFU for each dilution group. Data are presented as the average (±SD) for the total amount of CFU in each group of mice.

Long-Term Effect

Morbidity was monitored after receiving a single dose of PBS ($n = 4$), nontargeting siRNA ($n = 4$), or XCL1-targeting siRNA ($n = 4$). Mice were killed 180 days after receiving therapy, and *xcl1* transcript expression and the bacterial load in the lungs was determined as indicated above. Differences in the size of the lymphocytic foci between groups of mice were determined in H&E-stained lung sections. We used the diameter of the lymphocytic foci in 10× scale for at least 15 clusters per lobe of each mouse in each group. The data represent the average (±SEM) of lymphocyte foci diameter for mice treated with PBS, nontargeting siRNA, or XCL1-targeting siRNA.

Statistical Analysis

The data presented in this study are representative of results from three experiments. The data are expressed as the mean (±SEM) values ($n = 5$) from triplicate assays. The data have been analyzed using the Student's two-tailed t test for paired samples. P values less than 0.05 were considered significant.

RESULTS

Intrapulmonary Delivery of Aerosolized siRNA Is Confined to the Lungs

Because tuberculosis is a disease mainly confined to the lungs, our goal was to limit therapy to this organ. For this purpose, we first sought to determine whether delivery of fluorescent-tagged siRNA (Alexa 488-XCL1-targeting siRNA) could be found in other organs after intrapulmonary delivery of aerosolized siRNA.

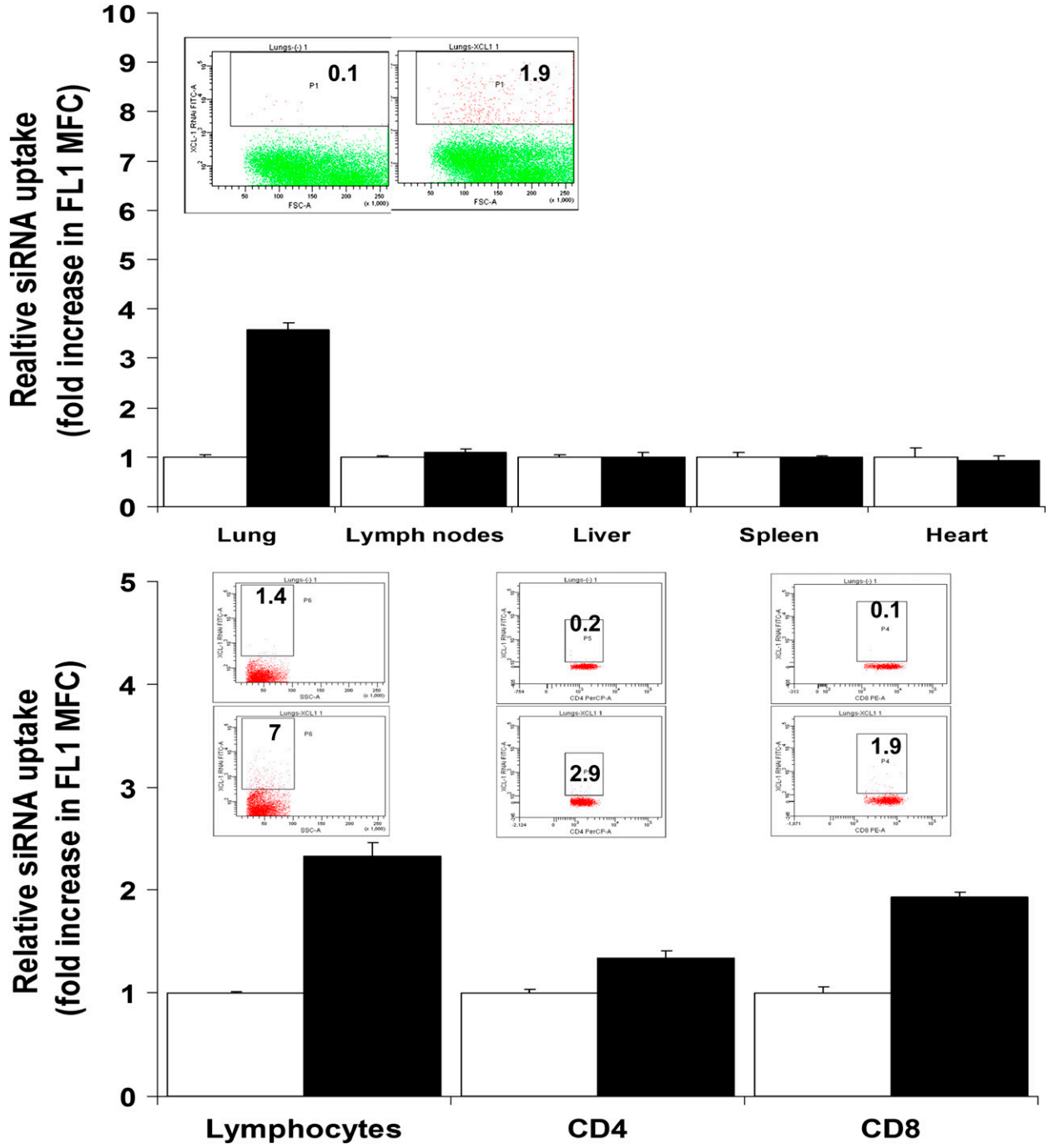

Figure 1. Intrapulmonary delivery of aerosolized small interfering RNA (siRNA) is confined to the lungs. Mice (C57BL/6 strain) were infected by low-dose aerosol challenge with *M. tuberculosis*. At 60 days of the infection, mice were treated via the intrapulmonary route with 15 μg of fluorescent-tagged siRNA (Alexa 488–XCL1-targeting siRNA). (*Upper panel*) Representative dot plots from lung samples. Numbers within the plots indicate the percentage of positive cells. Bar graph corresponds to the fold change in mean fluorescence channel (MFC), determined as the ratio of MFC in FL1 for samples obtained from mice treated with XCL1-targeting siRNA–Alexa 488 (*closed bars*), with the MFC in the same channel of cell suspensions obtained from the same organs of untreated mice (*open bars*). (*Lower panel*) Representative dot plots from lung samples. Numbers within the plots indicate the percentage of positive cells. The graph shows fold change in MFC determined as the ratio of MFC in FL1 for samples obtained from mice treated with XCL1-targeting siRNA–Alexa 488 (*closed bars*), with the MFC in the same channel of cell suspensions obtained from the same organs of untreated mice (*open bars*) after gating forward scatter/side scatter plot in the total lymphocyte gate followed by secondary gating in the CD4 or CD8 T–positive fluorescence.

Mice receiving 15 μg Alexa 488-siRNA targeting XCL1 were killed 24 hours after treatment. We prepared cell suspensions from the lungs, mediastinal lymph nodes, liver, heart, or spleen of each mouse. Thereafter, the cell suspensions were analyzed using flow cytometric analysis. We were able to demonstrate that, 24 hours after intrapulmonary delivery of XCL1-targeting siRNA, lung cell suspensions showed an increase in Alexa 488 relative fluorescence when compared with cells obtained from organs of untreated mice (Figure 1A).

XCL1 is mainly produced by activated CD8 T cells (20–24), including during chronic pulmonary tuberculosis (12). Thus, in the same experiment, we stained for CD8 and CD4 T cells to determine if the XCL1-targeting siRNA colocalized with target cells producing XCL1. Figure 1B shows that all populations of lymphocytes were positive for Alexa 488–siRNA, and also stained CD8 and CD4 T cells in mice treated with Alexa 488 XCL1-targeting siRNA.

Dose of siRNA

The optimal dose of siRNA was determined using three different concentrations of XCL1-targeting siRNA (5, 10, and 15 μg/mouse). Lung homogenates were obtained at 3 and 5 days after treatment, and XCL1 protein values were analyzed by ELISA. The results demonstrate that between 10 and 15 μg/mouse of siRNA were needed for maximum inhibition of XCL1 protein when compared with expression of XCL1 in mice receiving either nontargeting siRNA or PBS (hereafter termed control groups) (data not shown).

siRNA Targeting XCL1 Induced Transient Gene Silencing and Suppression of Protein Expression

Mice chronically infected with *M. tuberculosis* were given PBS, nontargeting siRNA, or XCL1-targeting siRNA. The percentage of *xcl1* gene silencing was determined by comparing levels of expression for this transcript between mice receiving XCL1-targeting siRNA and control groups. For this purpose, after one single dose, the levels of *xcl1* transcripts in each mouse were determined using qRT-PCR. Mice at 3 days after treatment with XCL1-targeting siRNA showed a 50% decrease in *xcl1* transcripts. However, when mice from the same group were evaluated 5 days after treatment, the expression of *xcl1* transcripts did not differ from control mice (Figure 2A). In addition, we investigated whether the silencing of the *xcl1 gene* translated into lower levels of XCL1 protein. The levels of XCL1 protein in the lungs were measured by ELISA using supernatants obtained from lung homogenates of each mouse at either 3 or 5 days after treatment. As shown in Figure 2B, mice receiving XCL1-targeting siRNA at 3 and 5 days after treatment had a 40–50% reduction in the levels of XCL1 protein, respectively, when compared with similar samples were obtained from control groups.

Reduced Expression of Pulmonary XCL1 Results in Changes in the Granulomatous Structure and Increased Fibrosis

We then determined whether gene silencing of *xcl1* and subsequent reduction in the expression of XCL1 affected the cell infiltration and histological makeup of the granulomatous response caused by pulmonary *M. tuberculosis* infection. For this purpose, lung tissue sections obtained from each mouse in each group were stained by H&E, and coded slides were evaluated by a pathologist. The histopathological analysis of these sections demonstrated less lymphocyte infiltration and less definition in the tuberculoid granuloma structure in XCL1-targeting siRNA–treated mice after 3 and 5 days of treatment when compared with control mice (Figure 3A). Moreover, it was noticed that the lungs from mice treated with XCL1-targeting siRNA were highly fibrotic when compared with control mice. Given this observation, the extent of fibrosis in these lesions was quantified by Masson's trichrome staining and computer-assisted image analysis. This analysis confirmed that the degree of fibrosis in mice treated with XCL1-targeting siRNA was two- to fourfold higher than in control mice (Figures 3B and 3E).

It is known that the cytokines, TGF-β and IL-4, are involved in the process of fibrosis (25, 26). Thus, we investigated whether the highly fibrotic areas of the tissue sections colocalized with the expression of any of these cytokines (Figures 3C and 3D).

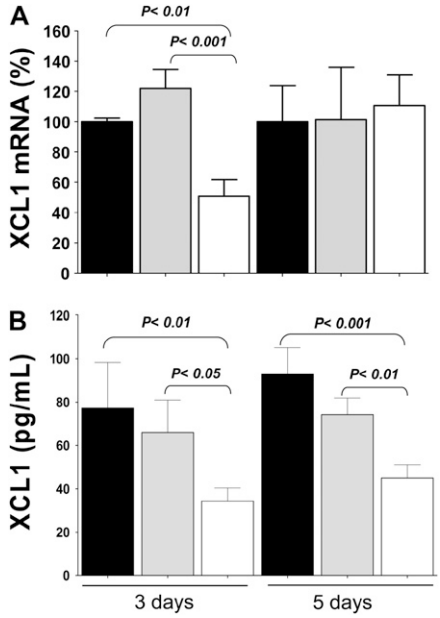

Figure 2. XCL1 gene silencing and protein suppression. (*A*) siRNA targeting XCL1 induced transient gene silencing and suppression of protein expression. After one single dose (15 μg/mouse) of XCL1-targeting siRNA (*open bars*), nontargeting siRNA (*gray bars*), or PBS (*closed bars*), the levels of *xcl1* transcripts in each mouse at 3 or 5 days after treatment were determined using quantitative RT-PCR. Mice at 3 days after treatment with XCL1-targeting siRNA had a 50% decreases in *xcl1* transcripts, but, 5 days after treatment, expression levels of *xcl1* transcripts were similar to those of control mice. (*B*) Levels of XCL1 protein. Mice receiving XCL1-targeting siRNA (*open bars*) at 3 and 5 days after treatment had a 40–50% reduction in the levels of XCL1 protein, respectively, when compared with similar samples obtained from control groups (*closed* and *gray bars*). Data presented represent the average (±SEM) of XCL1 mRNA (%) or XCL1 production from PBS, nontargeting siRNA, or XCL1-targeting siRNA.

IHC against TGF-β and IL-4 demonstrated that there was no such association between fibrosis and TGF-β or IL-4 expression. Despite a lack of colocalization with fibrosis, the IHC demonstrated that the pattern of expression of these two cytokines changed between groups. Thus, although TGF-β and IL-4 expression were clustered in the core of the granuloma in tissue sections from control mice, positive staining for these cytokines in sections from XCL1-targeting siRNA–treated mice were diffused throughout the lung tissue. Furthermore, it showed that many cells, such as lymphocytes, fibroblasts, macrophages, and dendritic cells, were positive for TGF-β and IL-4.

Lower Levels of Expression of Pulmonary XCL1 Are Associated with Decreased Numbers of CD4 and CD8 T Cells

The continuous presence of activated CD4 and CD8 T cells producing IFN-γ in chronically infected animals is an important element of this mouse model (27). Thus, the effect of *xcl1* gene silencing in these mice was evaluated by flow cytometry (Figure 4). This analysis demonstrated that the total numbers of CD4 and CD8 T cells were lower in XCL1-targeting siRNA–treated lungs when compared with similar samples obtained from control groups (Figures 4A and 4B). In mice treated with XCL1-targeting siRNA, the total number of CD4 T cells was reduced by 24–32% over the following 3–5 days. Likewise, the same mice showed a reduction of 20–40% in the total number of CD8 T cells. As expected, the numbers of cells expressing IFN-γ within

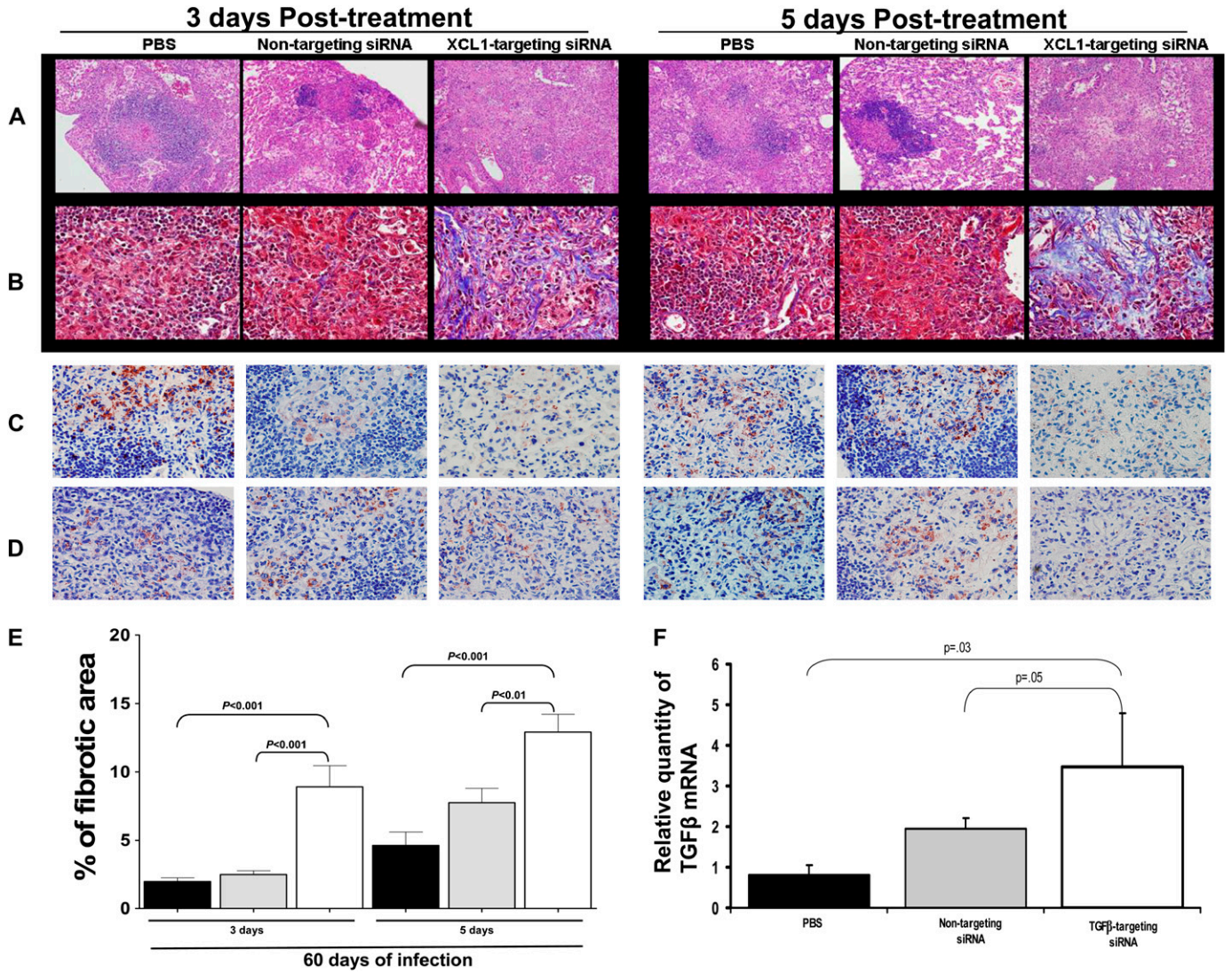

Figure 3. Reduced expression of pulmonary XCL1 results in changes in the granulomatous structure and increased fibrosis. (*A*) Images from lung tissue sections (10×) obtained from each mouse either at 3 or 5 days after treatment, stained by hematoxylin and eosin (H&E), and evaluated by a pathologist. The histopathological analysis of these sections demonstrated less lymphocyte infiltration and disruption of the tuberculoid granuloma structure in XCL1-targeting siRNA–treated mice after 3 and 5 days of treatment when compared with control mice (PBS or nontargeting siRNA). (*B*) Representative images (40×) from lung tissue sections obtained from each group stained by Masson's trichromic staining showing higher fibrosis in mice treated with XCL1-targeting siRNA at either 3 or 5 days after treatment. Immunohistochemistry (IHC) using antibodies to detect (*C*) transforming growth factor (TGF)-β and (*D*) IL-4 on tissue sections obtained from lungs of each mouse correlating with areas of fibrosis. The IHC demonstrated that there was no association between fibrosis and TGF-β or IL-4 expression (*red staining*). Expression of these two cytokines changed between groups; whereas TGF-β and IL-4 expression were clustered in the core of the granuloma in tissue sections from control mice, positive staining for these cytokines in sections from XCL1-targeting siRNA–treated mice were diffused throughout the lung tissue. Many cell types, such as lymphocytes, fibroblasts, macrophages, and dendritic cells, were positive for TGF-β and IL-4. (*E*) Quantitative image analysis of fibrosis using Masson's trichrome staining. The extent of fibrosis was quantified by Masson's trichrome staining and computer-assisted image analysis, as previously reported (18, 19). Positive blue signal, indicating collagen, was selected based on its color ranges, and the proportional area in each image was quantified using the histogram tool in Adobe Photoshop CS and expressed as a percentage of the image. Fibrosis in mice treated with XCL1-targeting siRNA (*open bars*) was two- to fourfold higher than in control mice (*gray* and *closed bars*). (*F*) Fold change of TGF-β mRNA expression compared with the housekeeping gene, GADPH, between lung samples obtained from chronically infected mice after 5 days of treatment with PBS (*closed bars*), nontargeting siRNA (*gray bars*), or XCL1-targeting siRNA (*open bars*). The relative levels of expression of TGF-β mRNA expression in the lungs at 5 days after treatment were significantly higher than in control mice.

the CD4 and CD8 T cells were also reduced by 27–50% and 28–42% in their respective cell populations (Figures 4A and 4B).

Lower Levels of Expression of Pulmonary XCL1 Results in Changes in the Expression of Microbicidal Mediators

IFN-γ is known to be essential to the control of bacterial growth in mice infected with *M. tuberculosis* (9, 10, 28). Thus, we studied whether transient pulmonary *xcl1* gene silencing at 60 days of the infection had any effect on the levels of IFN-γ expression. For this purpose, IFN-γ expression was measured by ELISA in supernatants obtained from lung homogenates of each mouse after treatment. We analyzed the data to determine the decrease in expression of IFN-γ for each group of XCL1-treated mice at 3 and 5 days, with their respective

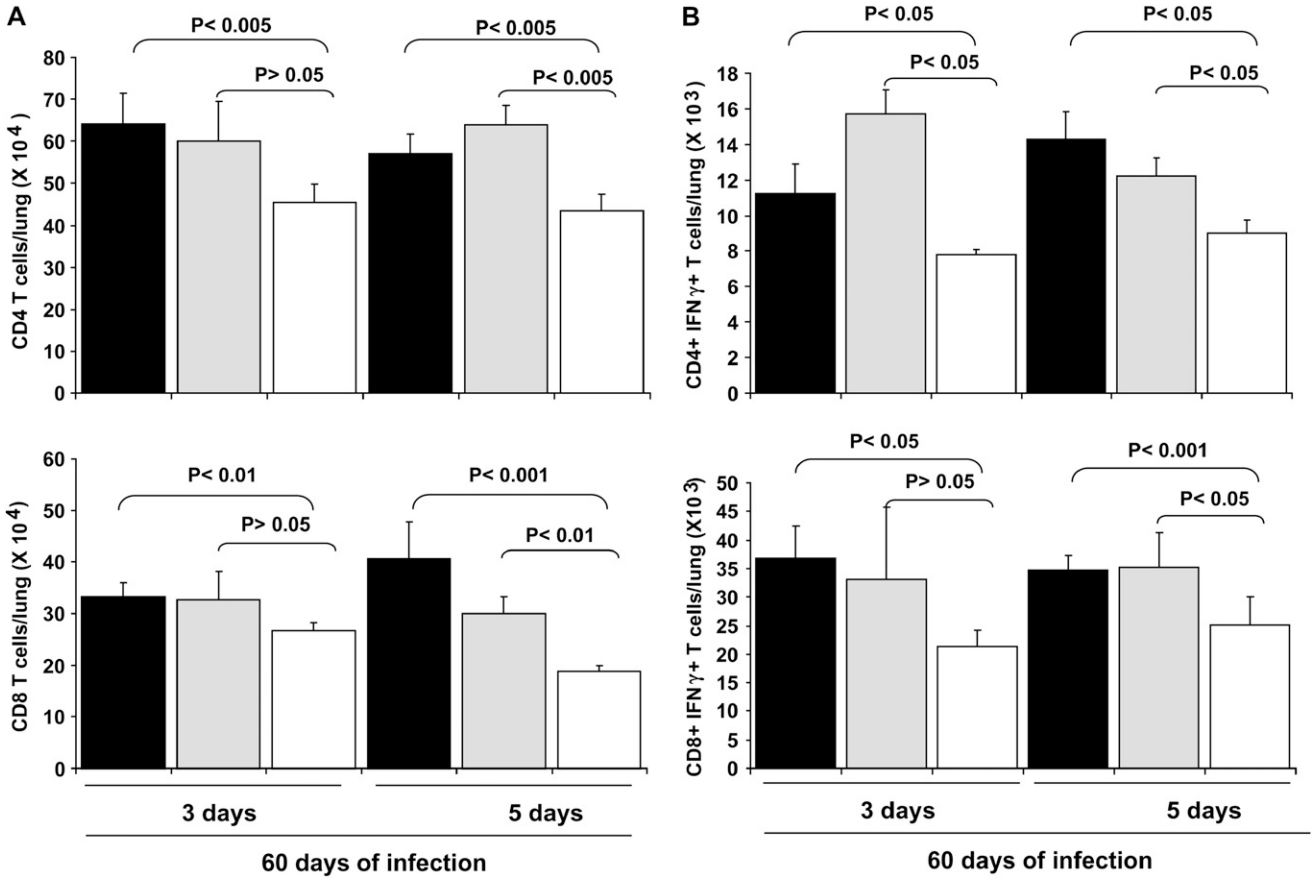

Figure 4. Lower levels of expression of pulmonary XCL1 are associated with decreased numbers of CD4 and CD8 T cells. (*A*) Numbers of total CD4 and IFN-γ expressing CD4 T cells were reduced in mice receiving XCL1-targeting siRNA (*open bars*) either at 3 or 5 days after treatment when compared with control mice (*closed* and *gray bars*). (*B*) The same mice showed a reduction of 18–50% in IFN-γ CD4 T cells, total number of CD8 T cells, and CD8 expressing IFN-γ T cells. Mice receiving XCL1-targeting siRNA (*open bars*) had a 20–40% and a 28–42% reduction in CD8 T cells and CD8 T cells expressing IFN-γ, respectively, when compared with control mice (*closed* and *gray bars*). Data are representative of three independent experiments and represent the average (±SEM) of CD4 and CD8, and CD4 and CD8 expressing IFN-γ from PBS (*closed bars*), nontargeting siRNA (*gray bars*), or XCL1-targeting siRNA (*open bars*).

controls. Accordingly, at 3 days after treatment, XCL1-targeting siRNA–treated mice had a decrease in IFN-γ expression of 32.8 and 41.1% when compared with similar samples obtained from PBS and nontargeting siRNA–treated mice, respectively. Similarly, at 5 days after treatment, XCL1-targeting siRNA–treated mice had a decrease in IFN-γ expression of 34 and 45% when compared with similar samples obtained from PBS and nontargeting siRNA–treated mice, respectively (Figure 5A).

Furthermore, IFN-γ is responsible for activating macrophages to produce antimicrobial substances, such as iNOS-activated NO (29, 30). The levels of expression of iNOS mRNA in the lungs at 3 days after treatment was decreased but had recovered by 5 days after treatment and was significantly greater then in control mice (Figure 5B). However, no changes were observed in the lung bacterial load after 3 to 5 days of treatment with XCL1-targeting siRNA treatment when compared with bacterial loads in control groups (Figure 5C).

Lower Levels of Expression of Pulmonary XCL1 Had a Long-Term Effect on the Lung Immunopathology

We asked whether intrapulmonary delivery of XCL1 targeting siRNA and short-term changes in the levels of XCL1 at 60 days after infection had a negative effect on the course of the pulmonary immunopathology. Thus, mice in all groups survived for at least 6 months after therapy. In these mice, we evaluated and compared the levels of *xcl1* transcripts, the histological makeup of the lungs and the bacterial load at 180 days after therapy. Surprisingly, at this time, mice that received XCL1-targeting siRNA therapy 180 days prior to analysis showed a 45% increase in the levels of *xcl1 gene* expression (Figure 6A), and the histological makeup differed from control groups (Figure 6B). In these mice, the lymphocytic foci in the lung parenchyma were larger than in control mice (Figures 6B and 6C). However, the fibrosis in XCL1-targeting siRNA was still slightly increased when compared with control mice (Figures 6C and 6D).

DISCUSSION

Recruitment of lymphocytes is a prominent feature of the inflammatory process in pulmonary tuberculosis. Here, we demonstrate that the expression of the chemokine, XCL1/lymphotactin, plays a role in the recruitment of T cells during the chronic stage of *M. tuberculosis* infection. To demonstrate this, we describe, for the first time, the manipulation of target gene expression at a specific time during chronic pulmonary

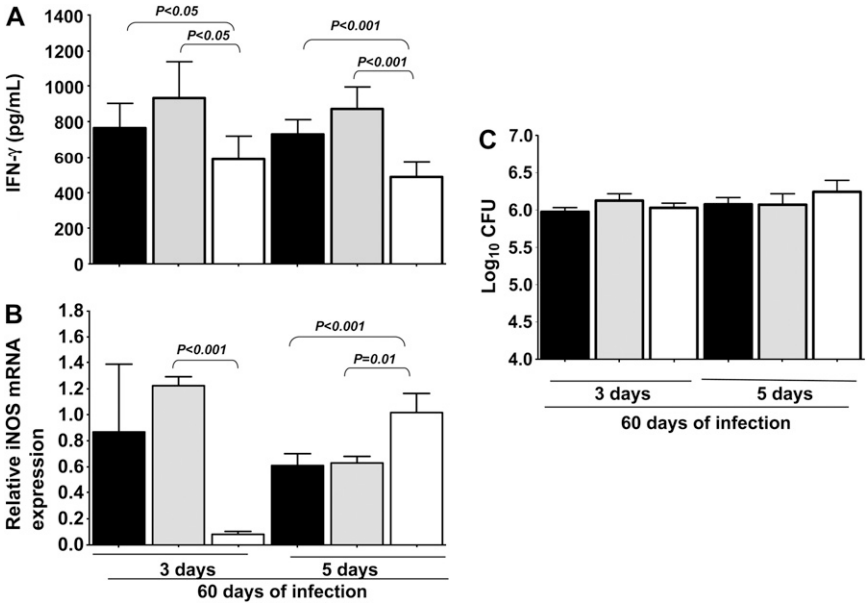

Figure 5. Lower levels of expression of pulmonary XCL1 results in reduced IFN-γ production. (*A*) Mice treated with XCL1-targeting siRNA (*open bars*), both at 3 or 5 days after treatment, had a one-third reduction in the total amount of IFN-γ protein when compared with similar samples obtained from control mice (*closed* and *gray bars*). (*B*) Fold change of inducible nitric oxide synthase (iNOS) mRNA compared with the housekeeping gene, GADPH, between lung samples obtained from chronically infected mice after treatment with PBS (*closed bars*), nontargeting siRNA (*gray bars*), or XCL1-targeting siRNA (*open bars*). The relative levels of expression of iNOS in the lungs at 3 days were lower, but recovered at 5 days after treatment. (*C*) Bacterial loads obtained from lung homogenates of chronically infected mice after treatment with PBS (*closed bars*), nontargeting siRNA (*gray bars*), or XCL1-targeting siRNA (*open bars*). Graphs are representative of three independent experiments, and represent the average (±SEM) of IFN-γ production, iNOS expression, and bacterial load from PBS, nontargeting siRNA, or XCL1-targeting siRNA.

infection. Here, we have combine our recently published non-invasive local pulmonary therapy (12, 14) with the recently developed technology of gene silencing mediated by siRNA (31–34) to study the role of the pulmonary XCL1/lymphotactin chemokine during chronic infection with *M. tuberculosis*.

Intrapulmonary delivery of naked and aerosolized XCL1-targeting siRNA appeared confined to the lungs, as we did not find siRNA-tagged Alexa 488 or changes in XCL1 protein expression in any of the peripheral or distant tissues screened (lymph nodes, heart, spleen, or liver). Furthermore, the siRNA appeared to be associated with CD8 T cells and, to some extent, with CD4 T cells as well. Previous work (12, 20, 21, 35) identified activated CD8 T cells as the main producers of XCL1 and, to some extent, natural killer and mast cell populations. We did not test for colocalization of siRNA with natural killer and mast cell populations; therefore, total suppression of *xcl1* transcript might not be limited to the CD8 T-cell population.

Local delivery of a single dose of XCL1-targeting siRNA was very efficient at reducing expression of both *xcl1* transcripts and XCL1 protein. However, these changes were only transient, because the levels of *xcl1* transcripts 5 days after treatment recovered to similar levels of expression found in control mice. As expected, a reduction in the expression of *xcl1* transcript was associated with a reduction in the levels of XCL1 protein at 3 days after treatment, and remained low at 5 days after treatment, even when the levels of *xcl1* transcript had already recovered.

The reduction in expression levels of XCL1 protein was associated with lower lymphocytic infiltration, both by histological analysis and by total lung CD4 and CD8 T-cell counts using flow cytometric analysis. These data suggest that XCL1 directly participates in the recruitment of T lymphocytes into the lung during chronic tuberculosis. Moreover, this also indicates that, during chronic infection, a continuous supply of XCL1 chemokine in the lungs is being provided, and that a temporary reduction of XCL1 chemokine at Day 60 of the infection is immediately reflected in a reduction in total T lymphocytes in the lungs. Furthermore, the focal lymphocytic aggregation in the granulomatous lesions was reduced in mice that had lower expression of XCL1. The data suggest that during the chronic stage of infection, pulmonary XCL1 also participates by driving/directing the T lymphocytes to the sites of inflammation. A similar finding was observed in our previous work (13), where transgenic mice overexpressing pulmonary granulocyte-macrophage colony–stimulating factor had reduced expression of XCL1 and appeared unable to direct lymphocytes to the granulomatous lesions.

A temporary reduction in XCL1 also changed the expression levels of total IFN-γ. Activated CD4 and CD8 T cells are the main source of IFN-γ during chronic infection with *M. tuberculosis* (12). Thus, the reduction in total IFN-γ levels was explained by decreased infiltration of total CD4 and CD8 T cells, which also resulted in reduction of numbers of CD4 and CD8 producing IFN-γ. Our previous studies (12), using intrapulmonary delivery of recombinant XCL1, indicated that high levels of expression of this chemokine did not affect the total number of CD4 and CD8 T cells present in the lungs, but resulted in a decreased number of CD4 T cells (but not CD8 T cells) producing IFN-γ. At that time, we hypothesized that a reduction in the levels of XCL1 would increase the numbers of CD4 T cells producing IFN-γ. However, the results from this study demonstrate that such reduction did not affect the CD4 T cells producing IFN-γ specifically but did affect the total CD4 T cell population. Altogether, this suggests that, whereas there is a critical level of XCL1 needed to recruit CD4 and CD8 T cells in the lungs, only high levels of XCL1 control the production of IFN-γ in the CD4 T cells. Previous studies suggest that XCL1 and its receptor, XCR1, may also act as a negative regulator of CD4 T cell activation, which points to a possible autocrine or paracrine regulation mechanism (23, 36); however, the precise mechanism is unknown.

The decreased XCL1 levels and subsequent decrease in IFN-γ expression in the lungs also affected the expression of iNOS transcripts for a short period of time. iNOS is an essential enzyme required for activation of microbicidal activity via NO production during chronic tuberculosis (30). The levels of iNOS transcripts after treatment followed a similar trend to that of the XCL1 transcripts. iNOS transcripts decreased at 3 days, but recovered rapidly at 5 days after treatment. We hypothesized that a significant drop in the expression of iNOS at 3 days after treatment should correlate with decreased antimicrobial activity and increased bacterial load. However, the bacterial load in the lungs of these mice did not change when compared with control mice at 3 or 5 days after treatment. These results may suggest

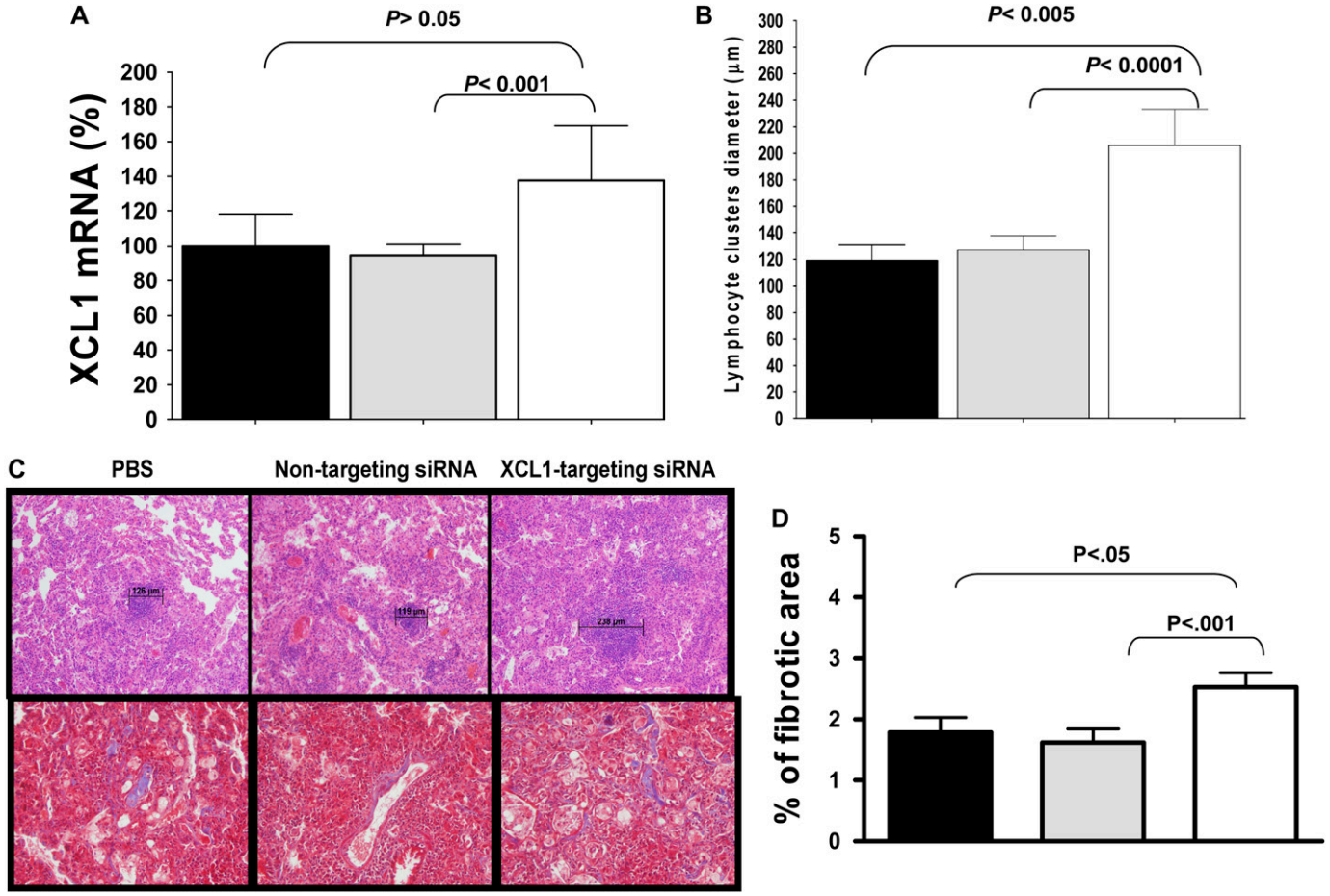

Figure 6. Lower levels of expression of pulmonary XCL1 had a long-term effect in the lung immunopathology. (*A*) Percentage of *xcl1* transcripts at 180 d after therapy in PBS (*closed bars*), non targeting siRNA (gray bars) or XCL1 targeting siRNA (*open bars*) treated mice. Mice that received XCL1-targeting siRNA had increased by 45% the levels of *xcl1* gene transcripts by 180 d after treatment. (*B*) Representative images of lymphocytic foci from each group. Bar indicates the size (μm) of lymphocytes foci in each sample. Images were taken using an Olympus BX41 microscope and DP70 camera. All images were obtained using a 10× objective. (*C*) For each group ($n = 5$), 25 randomly selected images (*upper panels*) of lymphocyte foci in H&E stained lung sections were measured in each group. Data represent the average (±SEM) of lymphocyte foci diameter for mice treated with PBS, nontargeting siRNA, or XCL1-targeting siRNA. The *lower panels* in (*C*) correspond to fibrosis determined by Masson's trichrome staining. (*D*) Quantitative image analysis of fibrosis using Masson's trichrome staining. The extent of fibrosis was quantified by Masson's trichrome staining and computer-assisted image analysis, as previously reported (18, 19). Positive *blue signal* in 25 images from each group, indicating collagen, was selected based on its color range, and the proportional area in each image was quantified using the histogram tool and expressed as a percentage of the image. Fibrosis in mice treated with XCL1-targeting siRNA was slightly higher than in control mice. Data are expressed as the mean (±SEM) values ($n = 25$). The data have been analyzed using Student's two-tailed *t* test for paired samples. *P* values less than 0.05 were considered significant.

that the timeframe of iNOS suppression was not sufficient to affect the bacterial load in the lungs, and that prolonged suppression of iNOS (and IFN-γ and XCL1) is needed to have an effect on the bacterial load.

Lower expression of XCL1 also affected lung fibrosis. In other studies, highly fibrotic areas correlated with increased TGF-β mRNA expression and with tissue colocalized with the expression of TGF-β and IL-4. In this study, we observed higher levels of TGF-β mRNA expression, but not IL-4 mRNA. However, the IHC staining demonstrated changes in the pattern of expression of both cytokines in the XCL1-targeting siRNA and control mice. These data, along with those of our early study, indicate an overall change in the inflammatory cell distribution associated with changes in the levels of XCL1 protein.

Finally, this transient therapy also demonstrates a much longer term effect on the immunopathological course of the chronic infection. After a transient but strong reduction of XCL1 around Day 60 of infection, the immune system appeared to overcompensate *xcl1* expression over a long period of time (180 days). Furthermore, increased levels of XCL1 led to larger lymphocytic foci in the parenchyma, indicating a role for XCL1 in the accumulation of lymphocytes at specific sites. These data support the concept that XCL1 participates in driving/directing lymphocytes to the site of infection. Interestingly, when using intrapulmonary delivery of recombinant XCL1 in our previous study, we also found that increased levels of XCL1 increased the size of these lymphocytic foci (12).

Immunotherapy is currently an important alternative in cancer and infectious diseases. As such, we demonstrate here, for the first time, in a murine tuberculosis model that it is possible to modulate the local environment and the lung immunopathology using siRNA. Currently, a variety of acute and chronic lung

diseases have shown to have altered expression of cytokines/chemokines or other important factors, many of them could be directly involved in the lung pathology. Therefore, workers on many other respiratory diseases will clearly be able to use the approaches described here to elucidate the role of different molecules in pathogenesis (12, 14). These same approaches may be exploited as immunotherapeutic alternatives for respiratory diseases.

Conflict of Interest Statement: None of the authors has a financial relationship with a commercial entity that has an interest in the subject of this manuscript.

Acknowledgment: The authors thank Dr. Alan Schenkel, Dr. Angelo Izzo, and Dr. Jeffrey Wilusz for reading the manuscript.

References

1. Shrivastava N, Srivastava A. RNA interference: an emerging generation of biologicals. *Biotechnol J* 2008;3:339–353.
2. de Fougerolles A, Vornlocher HP, Maraganore J, Lieberman J. Interfering with disease: a progress report on siRNA-based therapeutics. *Nat Rev Drug Discov* 2007;6:443–453.
3. de Fougerolles AR. Delivery vehicles for small interfering RNA *in vivo*. *Hum Gene Ther* 2008;19:125–132.
4. Bhandari V, Choo-Wing R, Lee CG, Zhu Z, Nedrelow JH, Chupp GL, Zhang X, Matthay MA, Ware LB, Homer RJ, *et al.* Hyperoxia causes angiopoietin 2–mediated acute lung injury and necrotic cell death. *Nat Med* 2006;12:1286–1293.
5. Lomas-Neira JL, Chung CS, Wesche DE, Perl M, Ayala A. *In vivo* gene silencing (with siRNA) of pulmonary expression of MIP-2 versus KC results in divergent effects on hemorrhage-induced, neutrophil-mediated septic acute lung injury. *J Leukoc Biol* 2005;77:846–853.
6. Matsuyama W, Watanabe M, Shirahama Y, Hirano R, Mitsuyama H, Higashimoto I, Osame M, Arimura K. Suppression of discoidin domain receptor 1 by RNA interference attenuates lung inflammation. *J Immunol* 2006;176:1928–1936.
7. Zhang X, Shan P, Jiang D, Noble PW, Abraham NG, Kappas A, Lee PJ. Small interfering RNA targeting heme oxygenase-1 enhances ischemia–reperfusion–induced lung apoptosis. *J Biol Chem* 2004;279:10677–10684.
8. WHO. Global tuberculosis control: surveillance, planning, financing. WHO report 2007. Geneva: World Health Organization; 2007. pp. 1–277.
9. Cooper AM, Flynn JL. The protective immune response to *Mycobacterium tuberculosis. Curr Opin Immunol* 1995;7:512–516.
10. Cooper AM, Roberts AD, Rhoades ER, Callahan JE, Getzy DM, Orme IM. The role of interleukin-12 in acquired immunity to *Mycobacterium tuberculosis* infection. *Immunology* 1995;84:423–432.
11. Rhoades ER, Cooper AM, Orme IM. Chemokine response in mice infected with *Mycobacterium tuberculosis. Infect Immun* 1995;63:3871–3877.
12. Ordway D, Higgins DM, Sanchez-Campillo J, Spencer JS, Henao-Tamayo M, Harton M, Orme IM, Gonzalez Juarrero M. XCL1 (lymphotactin) chemokine produced by activated CD8 T cells during the chronic stage of infection with *Mycobacterium tuberculosis* negatively affects production of IFN-gamma by CD4 T cells and participates in granuloma stability. *J Leukoc Biol* 2007;82:1221–1229.
13. Gonzalez-Juarrero M, Hattle JM, Izzo A, Junqueira-Kipnis AP, Shim TS, Trapnell BC, Cooper AM, Orme IM. Disruption of granulocyte macrophage–colony stimulating factor production in the lungs severely affects the ability of mice to control *Mycobacterium tuberculosis* infection. *J Leukoc Biol* 2005;77:914–922.
14. Higgins DM, Sanchez-Campillo J, Rosas-Taraco AG, Higgins JR, Lee EJ, Orme IM, Gonzalez-Juarrero M. Relative levels of M-CSF and GM-CSF influence the specific generation of macrophage populations during infection with *Mycobacterium tuberculosis. J Immunol* 2008; 180:4892–4900.
15. Delepine PMT, Guillaume C, Vaysse L, Le Pape A, Ferec C. Visualization of the transgene distribution according to the administration route allows prediction of the transfection efficacy and validation of the results obtained. *Gene Ther* 2002;9:736–739.
16. Bivas-Benita M ZR, Junginger HE, Borchard G. Non-invasive pulmonary aerosol delivery in mice by the endotracheal route. *Eur J Pharm Biopharm* 2005;61:214–218.
17. Gonzalez-Juarrero M, Orme IM. Characterization of murine lung dendritic cells infected with *Mycobacterium tuberculosis. Infect Immun* 2001;69:1127–1133.
18. Lehr HA, van der Loos CM, Teeling P, Gown AM. Complete chromogen separation and analysis in double immunohistochemical stains using Photoshop-based image analysis. *J Histochem Cytochem* 1999;47:119–126.
19. Yuan HT, Li XZ, Pitera JE, Long DA, Woolf AS. Peritubular capillary loss after mouse acute nephrotoxicity correlates with down-regulation of vascular endothelial growth factor-a and hypoxia-inducible factor-1 alpha. *Am J Pathol* 2003;163:2289–2301.
20. Blaschke S, Middel P, Dorner BG, Blaschke V, Hummel KM, Kroczek RA, Reich K, Benoehr P, Koziolek M, Muller GA. Expression of activation-induced, T cell-derived, and chemokine-related cytokine/lymphotactin and its functional role in rheumatoid arthritis. *Arthritis Rheum* 2003;48:1858–1872.
21. Cerdan C, Devilard E, Xerri L, Olive D. The C-class chemokine lymphotactin costimulates the apoptosis of human CD4(+) t cells. *Blood* 2001;97:2205–2212.
22. Dong C, Chua A, Ganguly B, Krensky AM, Clayberger C. Glycosylated recombinant human xcl1/lymphotactin exhibits enhanced biologic activity. *J Immunol Methods* 2005;302:136–144.
23. Kelner GS, Kennedy J, Bacon KB, Kleyensteuber S, Largaespada DA, Jenkins NA, Copeland NG, Bazan JF, Moore KW, Schall TJ, *et al.* Lymphotactin: a cytokine that represents a new class of chemokine. *Science* 1994;266:1395–1399.
24. Kennedy J, Kelner GS, Kleyensteuber S, Schall TJ, Weiss MC, Yssel H, Schneider PV, Cocks BG, Bacon KB, Zlotnik A. Molecular cloning and functional characterization of human lymphotactin. *J Immunol* 1995;155:203–209.
25. Hostettler KE, Roth M, Burgess JK, Gencay MM, Gambazzi F, Black JL, Tamm M, Borger P. Airway epithelium-derived transforming growth factor-beta is a regulator of fibroblast proliferation in both fibrotic and normal subjects. *Clin Exp Allergy* 2008;38:1309–1317.
26. Munitz A, Brandt EB, Mingler M, Finkelman FD, Rothenberg ME. Distinct roles for IL-13 and IL-4 via IL-13 receptor alpha1 and the type II IL-4 receptor in asthma pathogenesis. *Proc Natl Acad Sci USA* 2008;105:7240–7245.
27. Junqueira-Kipnis AP, Turner J, Gonzalez-Juarrero M, Turner OC, Orme IM. Stable T-cell population expressing an effector cell surface phenotype in the lungs of mice chronically infected with *Mycobacterium tuberculosis. Infect Immun* 2004;72:570–575.
28. Cooper AM, Dalton DK, Stewart TA, Griffin JP, Russell DG, Orme IM. Disseminated tuberculosis in interferon gamma gene–disrupted mice. *J Exp Med* 1993;178:2243–2247.
29. Cooper AM, Pearl JE, Brooks JV, Ehlers S, Orme IM. Expression of the nitric oxide synthase 2 gene is not essential for early control of *Mycobacterium tuberculosis* in the murine lung. *Infect Immun* 2000; 68:6879–6882.
30. Miller BH, Fratti RA, Poschet JF, Timmins GS, Master SS, Burgos M, Marletta MA, Deretic V. Mycobacteria inhibit nitric oxide synthase recruitment to phagosomes during macrophage infection. *Infect Immun* 2004;72:2872–2878.
31. Chang Z, Hu Z. RNAi therapeutics: can siRNAs conquer SARS? *Gene Ther* 2006;13:871–872.
32. DeVincenzo J, Cehelsky JE, Alvarez R, Elbashir S, Harborth J, Toudjarska I, Nechev L, Murugaiah V, Van Vliet A, Vaishnaw AK, *et al.* Evaluation of the safety, tolerability and pharmacokinetics of aln-rsv01, a novel RNAi antiviral therapeutic directed against respiratory syncytial virus (RSV). *Antiviral Res* 2008;77:225–231.
33. Durcan N, Murphy C, Cryan SA. Inhalable siRNA: potential as a therapeutic agent in the lungs. *Mol Pharm* 2008;5:559–566.
34. Li BJ, Tang Q, Cheng D, Qin C, Xie FY, Wei Q, Xu J, Liu Y, Zheng BJ, Woodle MC, *et al.* Using siRNA in prophylactic and therapeutic regimens against SARS coronavirus in rhesus macaque. *Nat Med* 2005;11:944–951.
35. Kim BO, Liu Y, Zhou BY, He JJ. Induction of c chemokine xcl1 (lymphotactin/single c motif-1 alpha/activation-induced, T cell–derived and chemokine-related cytokine) expression by HIV-1 tat protein. *J Immunol* 2004;172:1888–1895.
36. Middel P, Thelen P, Blaschke S, Polzien F, Reich K, Blaschke V, Wrede A, Hummel KM, Gunawan B, Radzun HJ. Expression of the T-cell chemoattractant chemokine lymphotactin in Crohn's disease. *Am J Pathol* 2001;159:1751–1761.